Carbohydrate Polymers 108 (2014) 281–290

Contents lists available at ScienceDirect

Carbohydrate Polymers

journal homepage: www.elsevier.com/locate/carbpol

Unrefined wood hydrolysates are viable reactants for the reproducible synthesis of highly swellable hydrogels

Laleh Maleki, Ulrica Edlund, Ann-Christine Albertsson*

Fiber and Polymer Technology, Royal Institute of Technology (KTH), Teknikringen 56, SE-100 44 Stockholm, Sweden

ARTICLE INFO

Article history:
Received 18 December 2013
Received in revised form 4 February 2014
Accepted 12 February 2014
Available online 28 February 2014

Keywords:
Hemicellulose
Biomass
Hydrogel
Renewable
Swelling
Wood hydrolysate

ABSTRACT

A value-adding robust and sequential synthetic pathway was elaborated to produce hydrogel structures with ionic character from crude acetylated galactoglucomannan-rich wood hydrolysate (WH). The WH was first-step liquor originating from a sulphite cracking pulp process for dissolving pulp. The synthetically modified WH fractions were verified at each step by NMR and FTIR, and the hydrogels were characterized with respect to their swelling and mechanical properties. Altering the crosslinking chemistry and the content of ionic moieties resulted in hydrogels with various swelling ratios and mechanical properties. Renewable hydrogel formulations with swelling ratios as high as $Q_{eq} = 270$ were achieved.

1. Introduction

Long-standing paper pulp mills are now evolving into biorefineries where an abundant renewable material is converted into energy and products. Aqueous process liquor side streams of the pulping industry, collectively known as wood hydrolysates (WHs), have recently been merited as versatile, low cost and viable renewable material feedstocks (Ragauskas et al., 2006). Although a growing trend in digital media has been partly replacing the traditional paper and printing market, and hence paper pulp production has faced a downward trend, there has been much effort to continue utilizing this ample renewable resource through other approaches.

There is a constant need for textiles by the ever-growing global population. Multiple environmental issues accompany cotton cultivation, such as the vast use of pesticides, high water consumption and relatively large areas of arable land required for cotton farms. These issues call for an urgent turnaround in cotton production. Today, there is an increasing demand for "dissolving pulp" as the most prominent resource for the production of cellulose derivatives and viscose. Dissolving pulp is a high cellulose content bleached wood pulp used in the textile industry and produced through an acid hydrolysis step (pre-hydrolysis) preceding the chemical pulping process (Sixta, 2006). Pre-hydrolysis aqueous fractions are fairly rich in heterogeneous oligo- and polysaccharides referred to as hemicelluloses, and contain some lignin. Such hemicellulose containing process liquors can also be obtained from other forestry processes, such as fiberboard production. A number of different methods for extracting and upgrading hemicellulose-rich process water from softwoods and hardwoods have been developed previously (Dahlman, Söderqvist Lindblad, Parkås, Albertsson & Edlund, 2009; Persson, Matusiak, Zacchi & Jönsson, 2006; Saadatmand, Edlund, Albertsson, Danielsson & Dahlman, 2012). Conventionally, fabrication of hemicellulose-based products, including barrier films and hydrogels, has focused on highly refined non-cellulosic polysaccharides (Albertsson, Voepel, Edlund, Dahlman & Söderqvist-Lindblad, 2010; Edlund & Albertsson, 2008; Hartman, Albertsson, Lindblad & Sjöberg, 2006; Söderqvist Lindblad, Ranucci & Albertsson, 2001). However, upgrading strategies render WHs utilization less economically feasible. We have recently demonstrated that crude or less purified WHs perform just as well as, or even superior to extensively upgraded counterparts in forming films with proper oxygen barriers and acceptable mechanical properties (Edlund, Ryberg & Albertsson, 2010; Ibn Yaich, Edlund & Albertsson, 2011; Saadatmand et al., 2013; Yaich, Edlund & Albertsson, 2014; Zhu Ryberg, Edlund & Albertsson, 2011).

Abbreviations: WH, wood hydrolysate; SWH, soft wood hydrolysate; APS, ammonium persulfate; KPS, potassium persulfate; MePro-Im, 1-[(1-imidazolyl)formyloxy]-2-methyl-2-propen; initiator *a*, redox initiator system comprising of KPS and sodium sulfite; initiator *b*, redox initiator system comprising of APS and sodium pyrosulfite; DAc, degree of acetylation; DS, degree of substitution.

* Corresponding author. Tel.: +46 8 7908274.
E-mail address: aila@kth.se (A.-C. Albertsson).

http://dx.doi.org/10.1016/j.carbpol.2014.02.060
0144-8617/

Non-cellulosic polysaccharide species are versatile in chemistry, and thanks to their abundance of pendant hydroxyl groups and inherent hydrophilicity together with biodegradability and nontoxicity, they can serve as potential substrates for hydrogel fabrication. Hydrogel formulations have been a targeted application owing to their capability as water, and general liquid absorbents in various applications, such as superabsorbents in hygiene products, drug delivery systems, water treatment, drying agents, and agriculture. Conventionally, most hydrogels are made from fossil-based polymers, but their growing popularity in a variety of applications necessitates the extended use of naturally occurring or renewable materials as reagents for hydrogel production. Relatively low cost access to a plentiful supply of hemicelluloses of different types, with properties fulfilling the requirements for hydrogel design, has turned hemicelluloses into an attractive natural resource. A number of pathways for producing hydrogels with refined hardwood (xylan) or softwood (*O*-acetyl-galactoglucomannan) hemicellulose core components have been suggested thus far (Edlund, Svensson & Albertsson, 2012; Kuzmenko, Hägg, Toriz & Gatenholm, 2013; Pahimanolis, Sorvari, Luong & Seppälä, 2013; Sun, Wang, Jing & Mohanathas, 2013; Söderqvist Lindblad, Albertsson, Ranucci, Laus & Giani, 2005). However, developing methodologies applicable to hemicellulose-containing fractions in a cruder state renders renewable products such as hydrogels more competitive and cost-efficient. Nevertheless, the synthetic pathway and applied chemistry must be further developed to meet the criteria of the demanding applications, in addition to competing with the existing fossil-based hydrogels in terms of mechanical properties, swellability and economics.

The delicacy of using biomass as a renewable resource arises from the dissimilarities among the hydrolysate fractions obtained from different processes. Process liquors, even though they are extracted from a specific type of wood, have many compositional differences, such as lignin content and purity, imposed by the cellulose recovery process. Therefore, enabling technologies for value-added wood components in biorefineries need to be versatile and robust to overcome any variations in the composition and purity of the biomass.

Our aim was to develop a robust, sequential synthetic pathway so that even cruder process liquor fractions are viable reactants for the reproducible synthesis of highly swellable hydrogel formulations with variable ionic charge. The ionic character of these hydrogels results in an appreciable water absorption and retention capacity. Our hypothesis was that process water fractions with *O*-acetyl-galactoglucomannan (AcGGM) as the major component derived from wood processing industries, although unrefined and containing lignin, can still be formulated into hydrogels with high degree of swelling and proper mechanical properties through a benign chemical pathway.

2. Experimental

2.1. Materials

N-N′-carbonyldiimidazole (CDI) 97% (Aldrich), acrylic acid (AA) anhydrous 99% (Aldrich), 2-methyl-2-propen-1-ol (MePro) (Aldrich), triethylamine (NEt_3) ≥ 99.9% (Fluka), chloroform (Fisher), dimethylsulfoxide (DMSO) 99.98% (Fisher), ethyl acetate 99.9% (VWR), sodium chloride ≥ 99.5% (Merck), hydrochloric acid 30% (Merck), potassium persulfate (KPS) ≥ 99.0% (Sigma), sodium sulfite anhydrous (Sigma), ammonium persulfate (APS) ≥ 98.0% (Sigma), sodium pyrosulfite ≥ 98% (Fluka), sodium sulfate 99.0% (Aldrich) were used as received.

The soft wood hydrolysates utilized in this work contained acetyl galactoglucomannan (AcGGM) as their main component and were obtained from hydrothermal treatment of spruce chips in two different processes. The first hydrolysate, herein denoted SWH1, was a first step liquor generated in a sulphite cracking pulp process for dissolving pulp, which was kindly provided by Domsjö Fabriker AB, Sweden. The second wood hydrolysate, denoted SWH2, was kindly supplied by Masonite AB, Rundvik, Sweden. SWH2 was a side product of the steam explosion of spruce wood chips, which was collected directly after the fiberboard machine prior to floatation. SWH1 was precipitated in ethanol and dried at 60 °C before use, whilst, SWH2 was subjected to centrifugation (20 min, 3600 rpm) followed by ultrafiltration. The membrane filtration was carried out to concentrate the waste liquor approximately 10 times, on a tangential flow filtration cartridge equipped with a cellulose membrane with a cutoff of 1000 Da (PLAC Prepscale, Millipore). The retentate (hemicellulose-rich fraction, 2 L) was further purified by diluting it in water to a volume of 10 L and then using diafiltration to concentrate the solution to 2 L. In the final step, the hemicellulose-rich retentate was freeze-dried.

2.2. Synthesis of 1-[(1-imidazolyl)formyloxy]-2-methyl-2-propen (MePro-Im)

1-[(1-Imidazolyl)formyloxy]-2-methyl-2-propen (MePro-Im) was prepared based upon a procedure previously described in literature (Voepel, Edlund & Albertsson, 2009). In a typical synthesis, 90 mmol (6.47 g) of 2-methyl-2-propen-1-ol (MePro) was dissolved in 40 mL chloroform, and 100 mmol (16.23 g) N-N′-carbonyldiimidazole (CDI) was added under stirring at room temperature. After 2 h, 40 mL of an aqueous HCl solution (pH 3) was introduced into the mixture to stop the reaction. The organic phase, containing the imidazolyl-activated compound, was extracted using a separation funnel and was washed repeatedly with 40 mL deionized water aliquots until the water phase reached a neutral pH. The chloroform-MePro-Im solution was subsequently dried using sodium sulfate for 1 h. After filtration, a solid product was acquired by rotary evaporation under reduced pressure.

2.3. Coupling of MePro-Im to wood hydrolysates

To produce allyl-modified wood hydrolysates, we used a similar procedure as previously presented by our group, with improvements to the synthesis of SWH1-MePro-Im by reducing the amount of DMSO and precipitating the product into ethyl acetate instead of 2-propanol (Voepel et al., 2009).

2.3.1. Preparation of allyl-modified SWH1 (SWH1-al)

5.73 mmol (0.9475 g = 1 equiv.) hexose units were dissolved in 30 mL DMSO. 165 μL (1.19 mmol, 0.2 equiv.) triethylamine (NEt_3) catalyst was added under stirring, and the mixture was placed in an oil bath at 50 °C. When the desired temperature was reached, 11.5 mmol (1.909 g = 2 equiv.) MePro-Im was added to the mixture and the reaction was allowed to proceed for 2, 4, 6 or 8 h. The reaction mixture was precipitated into cold ethyl acetate (0 °C, 400 mL), and the product was collected by centrifugation. The solid product was dried under vacuum for 24 h and re-dissolved in 8 mL DMSO followed by precipitation into 200 mL cold ethyl acetate (0 °C). The final product was obtained using centrifugation and dried under reduced pressure for 3 days.

2.3.2. Preparation of allyl-modified SWH2 (SWH2-al)

In a similar method to the synthesis of SWH1-al, 5.73 mmol hexose units of SWH2 were dissolved in 40 mL DMSO, and 165 μL NEt_3 was introduced into the solution. After raising the temperature to 50 °C, 11.5 mmol MePro-Im was added and allowed to react for 14, 20 or 40 h. The reaction mixture was then cooled and precipitated

Table 1
Composition of wood hydrolysate based hydrogels.

Modified SWH sample	Modified SWH (w/w)%	Acrylic acid (w/w)%	Initiator type	Initiator (w/w)%	Hydrogel formulation number	Denotation
SWH1-al_{24}	40	60	a[1]	3	1	SWH1-al_{24}/1a
	50	50	a	3	2	SWH1-al_{24}/2a
	60	40	a	3	3	SWH1-al_{24}/3a
SWH1-al_{36}	40	60	a	3	1	SWH1-al_{36}/1a
	50	50	a	3	2	SWH1-al_{36}/2a
	60	40	a	3	3	SWH1-al_{36}/3a
SWH1-al_{37}	40	60	a	3	1	SWH1-al_{37}/1a
	50	50	a	3	2	SWH1-al_{37}/2a
	60	40	a	3	3	SWH1-al_{37}/3a
SWH1-al_{38}	40	60	a	3	1	SWH1-al_{38}/1a
	50	50	a	3	2	SWH1-al_{38}/2a
	60	40	a	3	3	SWH1-al_{38}/3a
SWH1-al_{38}	40	60	b[2]	1	1	SWH1-al_{38}/1b
	50	50	b	1	2	SWH1-al_{38}/2b
SWH2-al_{29}	40	60	b	1	1	SWH2-al_{29}/1b
	60	40	b	1	3	SWH2-al_{29}/3b
SWH2-$al_{27\text{-}1}$	40	60	b	1	1	SWH2-al_{27}/1b
	60	40	b	1	3	SWH2-al_{27}/3b

[1] '*a*' Represents a redox initiation system consisting of potassium persulfate (KPS) and sodium sulfite.
[2] '*b*' Represents a redox initiation system consisting of ammonium persulfate (APS) and sodium pyrosulfite.

into 400 mL cold 2-propanol. A solid product was obtained by centrifugation followed by another precipitation and several washing steps before drying under vacuum to a constant weight.

2.4. Hydrogel synthesis from allyl-functionalized wood hydrolysates and acrylic acid

2.4.1. SWH1-based hydrogels

A number of SWH1-based hydrogels with various compositions were prepared from allyl-modified SWH1 with different modification times, according to the following method:

40/50/60 mg of the modified SWH1 corresponding to 40/50/60% of the final hydrogel's mass content was dissolved in 250 μL deionized water in glass vials (inner diameter 12 mm). Subsequently, 63/52.5/42 μL distilled acrylic acid (AA) (corresponding to 60/50/40% of the final hydrogel's mass content) was added under stirring. To this mixture, approximately 3 (w/w)% KPS and sodium sulfite were added as initiators, according to the total weight of AA and SWH1. After sufficient stirring, the glass vials were placed in an oven at 55 °C for 4 h until complete gelation was achieved. The cylindrical gels were recovered by breaking the glass vials, and they were placed in 100 mL deionized water for 24 h to extract unreacted compounds and initiators. The purified gels were dried for 4 days under a gentle stream of air.

In another experiment, SWH1-based hydrogels with 40 or 50% wood hydrolysate mass content were prepared by using 25 μL of an APS solution (40 g L^{-1}) in water and 25 μL of a sodium pyrosulfite solution (40 g L^{-1}) in water as the initiator, similar to the technique mentioned above.

2.4.2. SWH2-based hydrogels

Either 40 or 60 mg of SWH2-al with reaction times of 14, 20 or 40 h was dissolved in 250 μL deionized water in a glass mold (inner diameter 9 mm), and 60 or 40 mg distilled acrylic acid was added to this solution, respectively. To initiate the reaction, 25 μL of an APS solution (40 g L^{-1}) in water and 25 μL of a sodium pyrosulfite solution (40 g L^{-1}) in water were added to the mixture, and the molds were placed in an oven at 60 °C overnight. The resulting gels were retrieved by breaking the molds open and were placed in deionized water for 2 days to remove any impurities, before they were dried at room temperature and under vacuum.

2.5. Spectroscopy

Nuclear magnetic resonance (^{1}H NMR) was performed in $CDCl_3$ or DMSO-d_6 using a Bruker DMX-400 NMR operating at room temperature at 400 MHz. To measure the degree of acetylation (DAc) and the degree of allyl-substitution (DS), 50 mg of each vacuum-dried WH samples was dissolved in 0.75 mL DMSO-d_6 inside a glove box and under inert atmosphere. The solution was transferred into NMR tubes with a 5 mm outer diameter in nitrogen atmosphere.

The DAc was calculated from the relative integral of the acetyl group response at 2.02 ppm (I(Ac)) and the carbohydrate response at 3.2–5.6 ppm (I(carbohydrate)) according to Eq. (1): (Ibn Yaich et al., 2011).

$$\mathrm{DAc} = \frac{\mathrm{I(Ac)}/3}{\mathrm{I(carbohydrate)}/6} \quad (1)$$

The DS was calculated from the relative integral of the response from the methyl groups in the modified structure at 1.68 ppm ($I(CH_3)$) in relation to the previously calculated response of the acetyl groups at 2.02 ppm (I(Ac)), in accordance with Eq. (2): (Voepel et al., 2009).

$$\mathrm{DS} = \frac{\mathrm{I(CH_3)}/3}{\mathrm{I(Ac)}/3} \times \mathrm{DAc} \quad (2)$$

To facilitate data presentation and discussion, a labeling system has been adopted in which denotation of each sample depends on the SWH type, degree of allyl-substitution, composition of each hydrogel and the initiator system used. For instance, SWH1-al_{38}/1a refers to a hydrogel synthesized from SWH1 with an allyl-substitution degree of 38% (al_{38}), using hydrogel formulation number 1, and applying potassium persulfate and sodium sulfite as the redox initiation system (a), Table 1.

Fourier transform infrared spectroscopy (FTIR) measurements were performed on a Perkin–Elmer Spectrum 2000 equipped with an attenuated total reflectance (ATR) crystal accessory, within a range from 4000 cm^{-1} to 600 cm^{-1}. A mean of 16 scans at a 4 cm^{-1} resolution with atmospheric water and carbon dioxide correction

on each sample was recorded and evaluated by the Perkin–Elmer Spectrum software.

2.6. Swelling behavior of the WH-based hydrogels

2.6.1. Swelling ratio in deionized water

The swelling capacity of the SWH1-based gels in deionized water was assessed by immersing dry gel samples with a weight range between 30 and 50 mg in 100 mL deionized water. The gels were entrapped within stainless steel baskets with a mesh opening of 0.20 mm and an inner diameter of 30 mm. The weight gain of the gel samples was followed gravimetrically versus time after careful drying of the basket for each measurement. The swelling ratio (Q) was determined according to Eq. (3), in which m_0 refers to the initial weight of the gel in dry state, and m_t defines the weight of the gel at different times:

$$Q = \frac{m_t - m_o}{m_o} \quad (3)$$

The final swelling after 48 h is defined as Q_{eq}, and for each gel composition three individual samples were evaluated, and Q_{eq} is reported as the mean of these three individual assessments.

2.6.2. Swelling ratio in saline solution

The swelling behavior of the synthesized gels was also determined in 0.9% NaCl solution, according to the EDANA standard test WSP 241.2.R3 (EDANA, 2012). However, in this work the aforementioned stainless steel baskets were utilized instead of teabags suggested in the standard test. The general procedure of this test had a similar method to the determination of the swelling ratio in deionized water, except that m_t in Eq. (3) refers to the weight of the gel after 52 h.

To assess the influence of the ionic strength of the salt solution on the swelling behavior of the synthesized gels, the swelling ratio of SWH1-al$_{24}$/1a in a number of NaCl solutions with 0.1, 0.5, 0.9, 1.5, 2.0, 2.5, 3.0, 3.5 and 4% (w/w) salt concentration was measured. This measurement followed a similar method to the previously described procedure in which the equilibrium swelling refers to the swelling ratio after 52 h.

2.7. Characterization

Carbohydrate analysis was performed by sulfuric acid hydrolysis of the wood hydrolysates, according to TAPPI standard test T249 procedure. Although the obtained sugars were analyzed by ion exchange chromatography (IC) with a Dionex DX500 IC analyzer equipped with a Dionex GP50 gradient pump, an electrochemical detector (Dionex, ED40), Dionex PA1 separation column, and applying a sodium hydroxide/acetate buffer eluent.

Klason lignin content was determined by gravimetrically assessing the acid insoluble residues of the wood hydrolysates, in accordance with TAPPI standard method 222 (TAPPI, 2011).

Size exclusion chromatography was used to assess the molecular weight and polydispersity index of the wood hydrolysate samples. The characterization was performed on a Dionex Ultimate-3000 HPLC system (Dionex, Sunnyvale, CA, USA), equipped with an LPG-4300SD gradient pump, a WPS-3000SL autosampler and a DAD-3000 UV/Vis detector accompanied by a Waters-410 refractive index (RI) detector (Waters, Milford, MA, USA). The columns were a combination of three PSS suprema columns (300 mm × 8 mm, 10 μm particle size) with 30 Å, 1000 Å and 1000 Å pore sizes arranged in series together with a guard column (5 mm × 8 mm, 10 μm particle size). The SEC was calibrated using Pullulan standards with an Mp range of 342–708,000 Da (PSS, Germany). Sample solutions of 250 μL were injected for each measurement, and the mobile phase used was 10 mM NaOH at 40 °C with a flow rate of 1 mL/min.

Dynamic Mechanical Thermal Analysis (*DMTA*) Mechanical properties of the SWH1 hydrogels were investigated using a Q800 DMA analyzer (TA Instruments, USA) in compression mode. For this purpose hydrogel discs with approximately 15 mm diameter and 5 mm thickness were prepared. Each sample was soaked at room temperature (25 °C) for 1 min and heated to 60 °C with a temperature ramp of 5 °C/min and a frequency of 1 Hz.

Field Emission Scanning Electron Microscopy (*FE-SEM*) The topography and cross-section of the hydrogel samples were studied by a Hitachi s-4800 Field-Emission scanning electron microscopy with an acceleration voltage of 1.0 kV. The hydrogels in a dry or swollen state were immersed in liquid nitrogen and subsequently freeze-dried for 2 days prior to analysis. The samples were then mounted on stubs and sputter coated with a thin layer of gold/palladium using a Cressington 208HR High Resolution Au/Pd sputter.

3. Results and discussion

In line with the biorefinery concept, a method for valorizing the non-cellulosic fraction released to the process liquors in wood processing is derived. The not highly purified hemicellulose-rich wood hydrolysate (WH) was functionalized with alkenyl precursors and ionic moieties in a sequential synthetic scheme that affords covalent cross-linking. The crosslinking chemistry and the ionic strength was varied so that polymeric hydrogels with sufficient degree of swelling and mechanical performance were formed from crude raw materials.

3.1. Characterization of the hemicellulose-rich WH

The carbohydrate composition of SWH1 was determined to be 17% glucose, 45% mannose, 16% galactose and 8% arabinose, by the conditions described in TAPPI standard test T249 coupled with ion-exchange chromatography (IC)(TAPPI, 2009). SWH2 was composed of 10% glucose, 27% mannose, 17% galactose and 11% arabinose. In both cases, the WH was produced from spruce and the major hemicellulose fraction recovered is expected to consist of galactoglucomannan, which is sustained by the carbohydrate composition results. The Klason lignin content of the WHs was measured to be 0.6% and 4% for SWH1 and SWH2, respectively, according to TAPPI standard method 222 (TAPPI, 2011). Molecular weight analysis of SWH1 and SWH2 using size exclusion chromatography showed a number average molecular weight of approximately 3500 g mol^{-1} and a polydispersity index (Đ) of 1.95 for SWH1, and a number average molecular weight of 900 g mol^{-1} and a Đ value of 1.9 for SWH2.

3.2. Preparation of allyl-functionalized wood hydrolysate

To allow for subsequent crosslinking, allyl groups were in a first step introduced onto the hemicellulose backbone according to Scheme 1. This reaction consists of a coupling reaction between hydroxyl groups on the polysaccharide molecules in the wood hydrolysate and 1-[(1-imidazolyl)formyloxy]-2-methyl-2-propen as the coupling precursor in DMSO at 50 °C in the presence of NEt_3 as a catalyst. The modification reaction was carried out for 2, 4, 6 or 8 h to investigate the influence of the reaction time on the degree of substitution.

The degree of substitution on the modified samples was evaluated by ^{1}H NMR spectroscopy: the integral of the methyl protons of the vinylic derivative at 1.68 ppm was compared to the response of the acetyl group at 2.02 ppm. The ^{1}H NMR spectra of crude SWH1 along with the four modified SWH1 samples is shown in Fig. 1, demonstrating both the appearance of the aforementioned peak

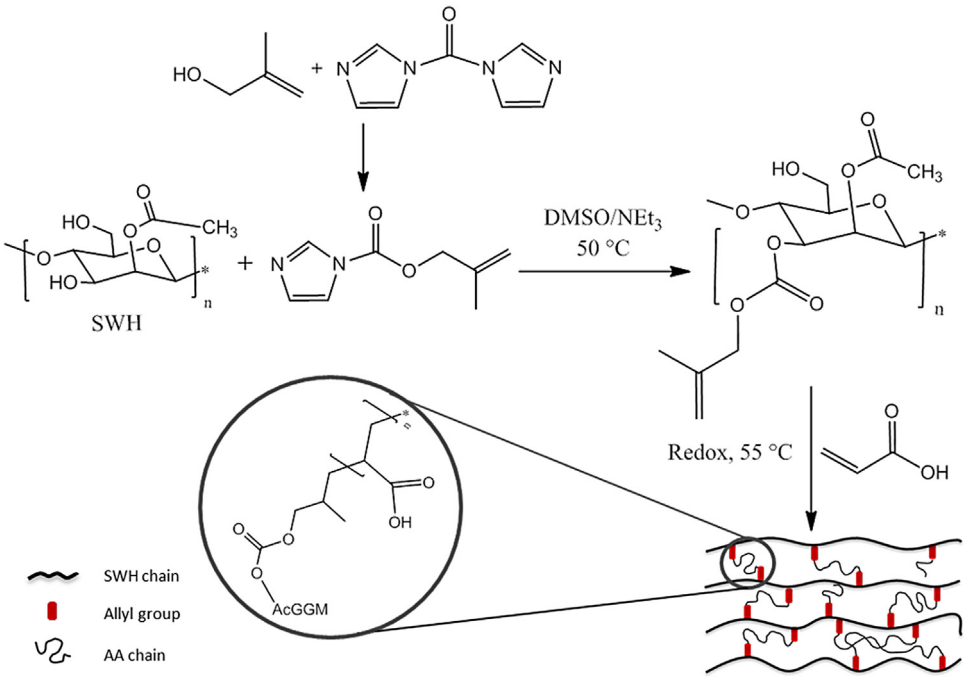

Scheme 1. General synthetic scheme for WH-based hydrogels.

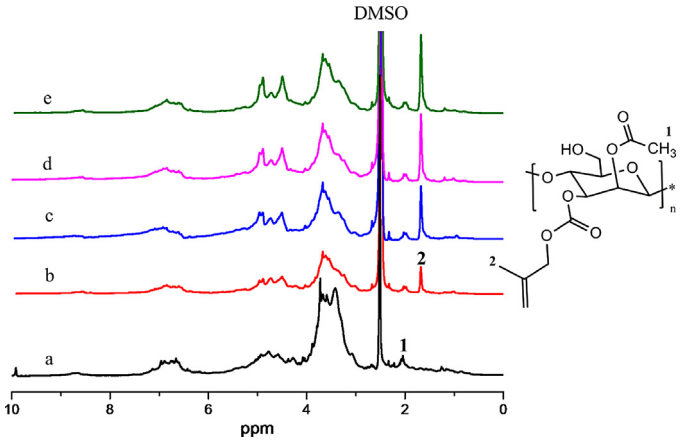

Fig. 1. ^{1}H NMR spectra of: (a) crude SWH1 and modified for (b) 2 h, (c) 4 h, (d) 6 h and (e) 8 h.

at 1.68 ppm and an increasing trend in the intensity of the methyl protons versus reaction time. However, according to the calculated degrees of substitution, Table 2, substitution of the hydroxyl protons has reached an approximate plateau after 4 h of reaction. In the design of this synthetic pathway, it was targeted to not only use a sustainable raw material, but also perform all the synthetic steps at ambient conditions if possible and avoid demanding and costly steps such as vacuum drying, degassing or inert atmospheres. Hence, traces of water are present in the reaction vessel during the allyl coupling reaction, which may have caused unavoidable side reactions and leading the degree of substitution to level off after 4 h of reaction.

Table 2
Degrees of substitution and denotation of allyl-modified SWH1 with varying reaction time obtained by ^{1}H NMR.

Denotation	Reaction time (h)	Average degree of substitution (DS)
SWH1-al$_{24}$	2	0.24
SWH1-al$_{36}$	4	0.36
SWH1-al$_{37}$	6	0.37
SWH1-al$_{38}$	8	0.38

During NMR analysis however, samples were prepared under inert conditions to allow for accuracy of the DAc and the DS calculations. It is noteworthy that no trace of water peak at approximately 3.30 ppm was observed due to the thorough NMR investigation and the use of glovebox.

To confirm the covalent attachment of the acrylated compound to the hemicellulose, FTIR spectroscopy was also applied and the emergence of a new peak at 1745 cm^{-1}, due to the C=O stretching of the allyl-SWH1, was evidence for a successful covalent coupling, Fig. 2. (Socrates, 2001) The attached MePro moiety also resulted in another peak at approximately 952 cm^{-1}, attributed to CH_2 out-of-plane wagging; however, the characteristic polysaccharide bands may have concealed other characteristic peaks of MePro.

3.3. Hydrogel synthesis from allyl-functionalized SWH1 through redox initiation

Hydrogels of varying compositions were prepared by dissolving the desired amounts of allyl-modified SWH1 together with acrylic acid in water and initiating the polymerization by potassium persulfate and sodium sulfite as a redox initiation system. In a comparative experiment, two additional groups of hydrogels were prepared by replacing the former initiators with ammonium persulfate and sodium pyrosulfite. All the hydrogels were prepared in a cylindrical shape, and they had brownish color stemming from the original wood hydrolysate. These gels were soft in the swollen state in water but hard and brittle in the dry state.

The formation of covalently bonded hydrogels containing oligoacrylic acid bridges was investigated by comparing the FTIR spectra of crude SWH1, SWH1-al and the corresponding hydrogel, Fig. 2. In the FTIR spectrum of pristine SWH1, a broad band at 3000–3500 cm^{-1} represents the OH stretching of the hydroxyl groups present in the backbone of hemicellulose, and the depression in the intensity of OH stretching in SWH1-al$_{38}$ spectrum is evidence for some hydroxyl groups being substituted by an allyl

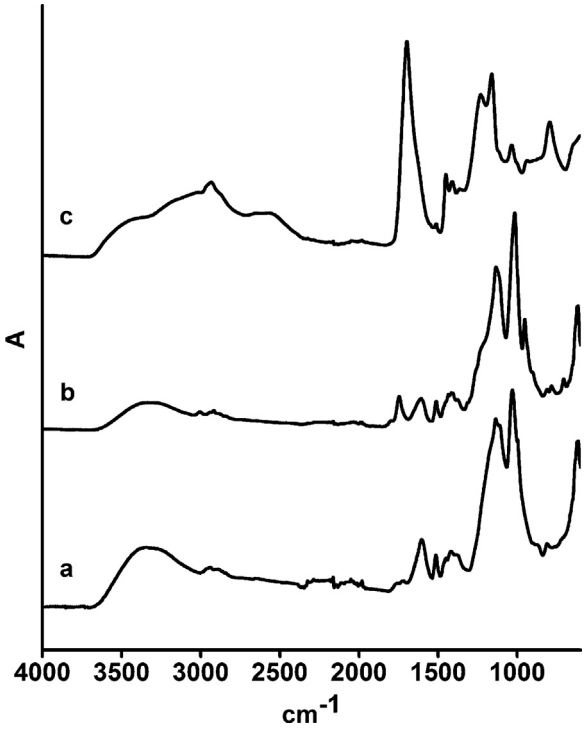

Fig. 2. FTIR Spectra (wavenumber versus absorption) of (a) crude SWH1, (b) modified SWH1-al$_{38}$ (DS = 0.38) and (c) SWH1-al$_{38}$/1a hydrogel.

group. The attachment of the modifying groups to SWH1 also resulted in the emergence of a peak at 1746 cm^{-1}, stemming from the stretching mode of the C=O groups in the covalently bonded allyl group. An absorption at 1606 cm^{-1} is attributed to a C=C stretching vibration of vinylidene in the spectrum of the modified species; however, the disappearance of this signal in SWH1-al$_{38}$/1a shows a considerable number of the C=C double-bonds attached to the AcGGM chain have participated in the covalent creation of a three-dimensional network. The formation of hydrogels containing oligomeric chains of poly acrylic acid can also be proven by the appearance of a high intensity peak near 1695 cm^{-1} as a result of C=O stretching of the carboxylic acid functional group in the acrylic acid backbone.

3.4. Hydrogel swelling properties

Evaluation of hydrogel swelling behavior was performed by placing each synthesized gel in an excess of deionized water and following the weight gain gravimetrically over a period of 48 h. Swelling curves of the hydrogels with three distinct compositions made from SWH1-al$_{24}$ and SWH1-al$_{38}$ are shown in Fig. 3-I. Regardless of the degree of substitution, formulations containing 60 (w/w)% acrylic acid show superior swelling (Q_{eq} = 172 for SWH1-al$_{24}$/1a and Q_{eq} = 91 for SWH1-al$_{38}$/1a), which is attributed to the contribution of the ionizable concomitant pendant hydroxyl side groups of polyacrylic acid chain to the swelling process, in addition to the hydrophilic functional groups' interaction with water. Poly(acrylic acid) has a pKa of 6.8 and is well capable of deprotonation and ionization in deionized water (Mittal & Anderson, 2000). Due to the presence of the ions within the hydrogel and the difference between ion concentration inside the gel and the surrounding medium, osmosis pressure can enhance hydrogel swelling (Hossein & Kinam, 2010). As the acrylic acid content of the hydrogels is decreased, osmosis has a smaller share of the swelling forces and more dominant water-hydrophilic polymer interaction leads to smaller swelling ratios for the other hydrogel formulations.

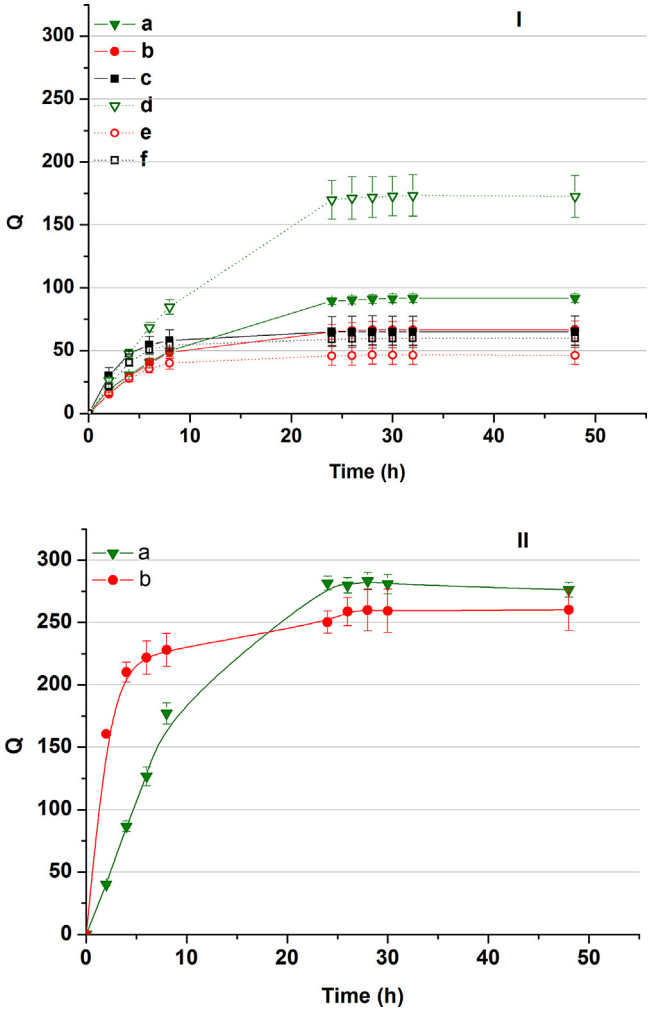

Fig. 3. (I) Swelling of SWH1 – based hydrogels in deionized water (a) SWH1-al$_{24}$/1a, (b) SWH1-al$_{24}$/2a, (c) SWH1-al$_{24}$/3a, (d) SWH1-al$_{38}$/1a, (e) SWH1-al$_{38}$/2a and (f) SWH1-al$_{38}$/3a. (II) Swelling of (a) SWH1-al$_{38}$/1b and (b) SWH1-al$_{38}$/2b.

Nevertheless, all the formulations with less than 60 (w/w)% acrylic acid content display swelling values of at least Q = 50, which is a highly valuable feature in many applications.

Swelling curves of hydrogels synthesized using APS and sodium pyrosulfite (initiator *b*) with two different compositions is presented in Fig. 3-II. By comparing this plot to the swelling curves of SWH1-al$_{38}$ in Fig. 3-I, a large variation in swelling ratio can be observed, although all hydrogels have been produced from modified wood hydrolysate with similar degrees of substitution. This variation can be explained by the difference in the performance of the two particular redox initiator systems. Remarkably higher swelling ratios of SWH1-al$_{38}$/1b and SWH1-al$_{38}$/2b compared to SWH1-al$_{38}$/1a and SWH1-al$_{38}$/2a with identical compositional proportions indicate a lower crosslink density of the hydrogels synthesized with initiator *b*, which is further confirmed by comparing their mechanical properties.

The repeated swelling-deswelling behavior of hydrogels is an essential factor for some applications, and a key element to demonstrating the true network structure of a hydrogel. Fig. 4 shows the swelling curves of SWH1-al$_{24}$/1a after three consecutive swelling-drying cycles. SWH1-al$_{24}$/1a, which possesses the lowest degree of substitution, reached a swelling degree of approximately 150 after both the second and the third swelling cycle without any disintegration of the structure.

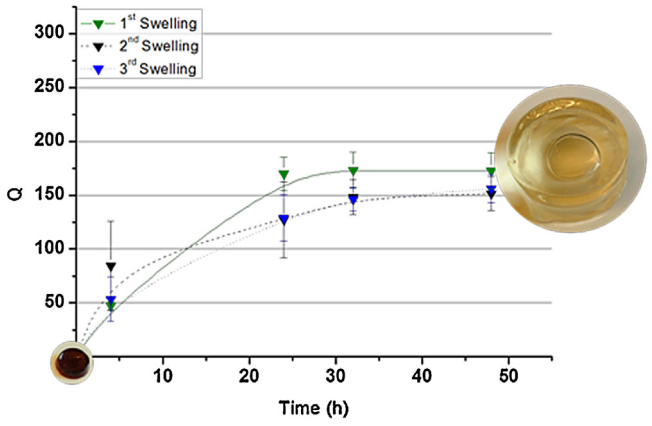

Fig. 4. Swelling curves of SWH1-al$_{24}$/1a hydrogel in deionized water after three consecutive swelling-drying cycles.

3.5. Swelling of SWH1 hydrogels in 0.9% saline solution

For some hydrogel applications, water retention capacity in the presence of external ions is of great significance. Hydrogels used in agricultural and horticultural applications are intended to absorb water along with fertilizers and other nutrients. Moreover, an established standard method to assess the fluid retention capacity of hydrogels designed for hygiene products is based upon swelling of hydrogels in predetermined concentrations of saline solution (EDANA, 2012). In Fig. 5, the swelling curves in 0.9% saline solution of the three different formulations of SWH1-al$_{24}$ and SWH1-al$_{38}$ synthesized using initiator *a* are plotted over 52 h. According to the results, all the hydrogels have experienced a dramatic decrease in their equilibrium swelling in saline solution compared with their equilibrium swelling in deionized water. As it has been mentioned before, electrostatic interactions and osmosis pressure serve as the main driving force for the swelling of hydrogels containing dissociable ionic pendant groups. In saline solution, a low molecular weight electrolyte can travel into the gel structure, and the counter ion introduces a screening effect on the carboxylate anions. This shielding effect not only reduces the anion-anion repulsion of carboxylates but also lessens the difference in salt concentration in the vicinity of the gel structure and in the surrounding medium, eventually leading to lower osmosis pressure and reduced equilibrium swelling (Mun, Suleimenov, Park & Omidian, 2010).

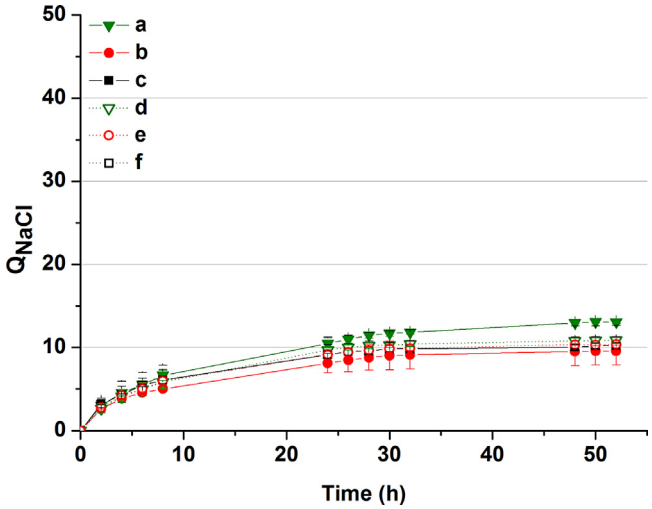

Fig. 5. Swelling curves of (a) SWH1-al$_{24}$/1a, (b) SWH1-al$_{24}$/2a, (c) SWH1-al$_{24}$/3a, (d) SWH1-al$_{38}$/1a, (e) SWH1-al$_{38}$/2a and (f) SWH1-al$_{38}$/3a in 0.9% NaCl.

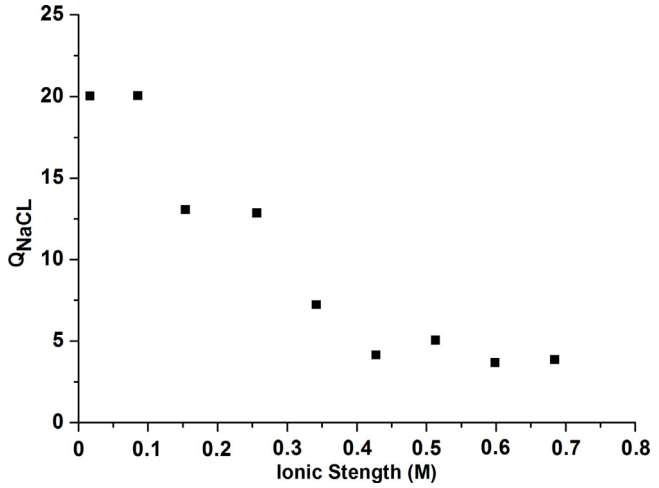

Fig. 6. Equilibirum swelling of SWH1-al$_{24}$/1a as a function of the ionic strength of the aqueous swelling medium.

Since the hydrogels swell significantly less in 0.9% saline solution than in deionized water, there might be shrinking effect with increasing ionic strength, which could be of interest in certain applications. In Fig. 6, the equilibrium swelling value of SWH1-al$_{24}$/1a in saline solutions of varying NaCl concentration is plotted against the salt concentration in % (w/w). It is observed that with increasing NaCl concentration, the equilibrium swelling ratio decreases until a gel shrinkage point is reached. This decrease in swelling ratio also arises from the higher concentration of the free ions within the vicinity of the gel.

3.6. Thermo-mechanical properties of SWH1-based hydrogels

Dynamic mechanical thermal analysis (DMTA) was used to assess the mechanical performance of the hydrogels synthesized from SWH1 over a broad temperature range. DMTA assessments provide valuable information on the thermorheological properties of the hydrogel systems, such as storage modulus, loss modulus and damping at various temperatures. The different SWH1 hydrogels, synthesized using the two previously mentioned initiators (*a* and *b*), were subjected to compressive deformation at a frequency of 1 Hz and with constant amplitude over a wide temperature spectrum. The obtained storage moduli (E') and damping (tan(δ)) values of the hydrogels at room temperature and 60 °C are tabulated in Table 3.

All hydrogels show a slight decreasing trend in their storage moduli as the temperature was raised to 60 °C (Fig. 7), which was attributed to the loss of water. Furthermore, all hydrogels of varying compositions presented higher storage moduli (E') than loss moduli in the selected temperature window, which indicates that the elastic response of the gels predominates their viscous response, even at temperatures as high as 60 °C. Hydrogels prepared using initiator *b* have a lower E' compared to the hydrogels prepared with initiator *a*. As the mechanical strength of hydrogels is strongly influenced by the degree of cross-links in the system, this difference in mechanical properties is another indication of the lower cross-link density of the b-series hydrogels (Anseth, Bowman & Brannon-Peppas, 1996).

Comparing all of the hydrogels prepared using initiator *a* showed that the variations in the weight percentage of acrylic acid has not imposed a dominant impact on the mechanical properties. Nevertheless, all the attained hydrogels possess sufficiently high strength to function as absorption components.

Table 3
Storage moduli and damping of SWH1 hydrogels at room temperature and 60 °C obtained by DMTA.

Sample	E'(kPa) at room temperature	tan(δ) at room temperature	E'(kPa) at 60 °C	tan(δ) at 60 °C
SWH1-al$_{24}$/1a	8.83	0.42	8.57	0.35
SWH1-al$_{24}$/2a	5.64	0.18	4.81	0.24
SWH1-al$_{24}$/3a	10.05	0.25	6.92	0.29
SWH1-al$_{36}$/1a	15.69	0.16	11.22	0.14
SWH1-al$_{36}$/2a	3.90	0.16	3.34	0.10
SWH1-al$_{36}$/3a	6.50	0.24	5.57	0.20
SWH1-al$_{37}$/1a	6.39	0.25	5.42	0.20
SWH1-al$_{37}$/2a	9.19	0.15	9.09	0.16
SWH1-al$_{37}$/3a	9.95	0.37	8.71	0.35
SWH1-al$_{38}$/1a	8.00	0.10	6.64	0.12
SWH1-al$_{38}$/2a	5.05	0.13	4.19	0.14
SWH1-al$_{38}$/3a	0.51	0.24	0.21	0.31
SWH1-al$_{38}$/1b	1.29	0.14	1.20	0.14
SWH1-al$_{38}$/2b	2.56	0.10	1.69	0.15

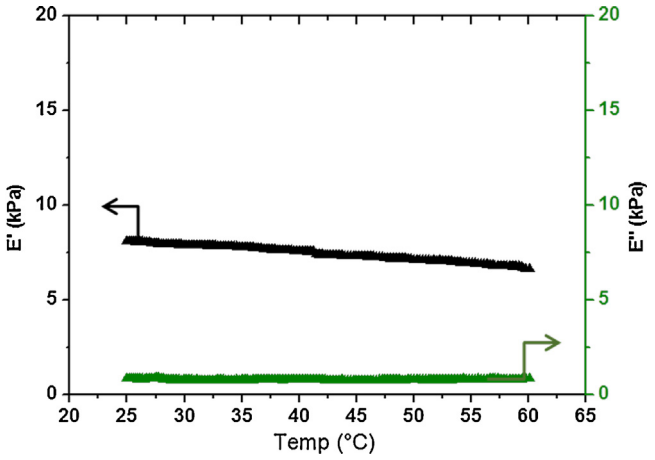

Fig. 7. Storage (E') and loss (E'') moduli of SWH1-al$_{38}$/1a, acquired from DMTA.

3.7. Morphological studies of the SWH1 hydrogels

To better investigate the formation of a network structure and the effect of swelling on the morphology of the hydrogels, dry and swollen SWH1-al$_{24}$/1a hydrogels were lyophilized and subsequently examined by SEM. SEM micrographs of the surfaces and cross-sections of SWH1-al$_{24}$/1a in the dry state, equilibrium swelling in 0.9% saline solution and equilibrium swelling in deionized water are presented in Fig. 8. By comparing Fig. 8-a, -b and -c, topological alterations relative to the degree of equilibrium swelling can be observed. Although, lyophilization can contribute to the formation of the porous structure observed in the SEM images, expansion of the hydrogel as a result of swelling is clearly noticeable in Fig. 8-d and -e. Furthermore, Fig. 8-e is valuable evidence indicating the presence of a three-dimensional structure in the hydrogel formulations with the highest equilibrium swelling ratio.

3.8. Robustness and versatility of the hydrogel synthesis pathway

Adaptability of this hydrogel manufacturing technique to other wood hydrolysates was investigated by applying the previously described protocol on another soft wood hydrolysate (SWH2). SWH2 was derived from steam explosion of spruce wood chips in fiberboard production, and due to the different cellulose recovery process, it is richer in lignin content and the average molecular weight of the remaining hemicellulose chains is lower. Allyl-coupling to an AcGGM chain of SWH2 was performed following the procedure illustrated in Scheme 1; however, the reaction time

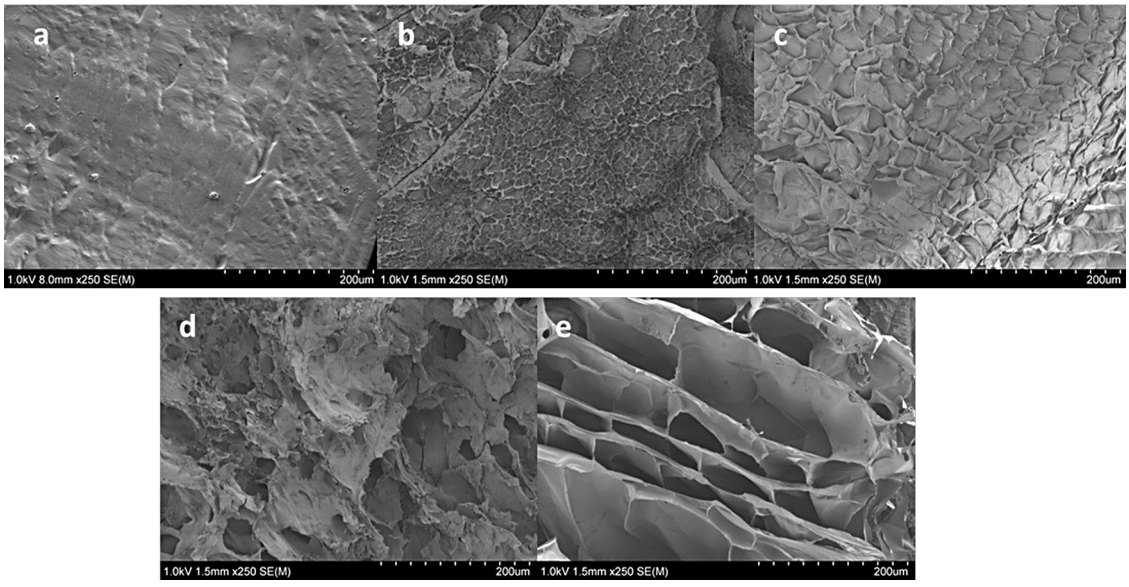

Fig. 8. SEM images (250× magnification) of the surface of (a) dry SWH1-al$_{24}$/1a, (b) SWH1-al$_{24}$/1a swollen in NaCl, (c) SWH1-al$_{24}$/1a swollen in deionized water, and the cross-section of (d) SWH1-al$_{24}$/1a swollen in NaCl and (e) SWH1-al$_{24}$/1a swollen in deionized water.

Table 4
Degree of substitution of allyl-modified SWH2 after 14, 20 and 40 h of reaction obtained by ^{1}H NMR.

Denotation	Reaction time (h)	Average degree of substitution (DS)
SWH2-al$_{29}$	14	0.29
SWH2-al$_{27\text{-}1}$	20	0.27
SWH2-al$_{27\text{-}2}$	40	0.27

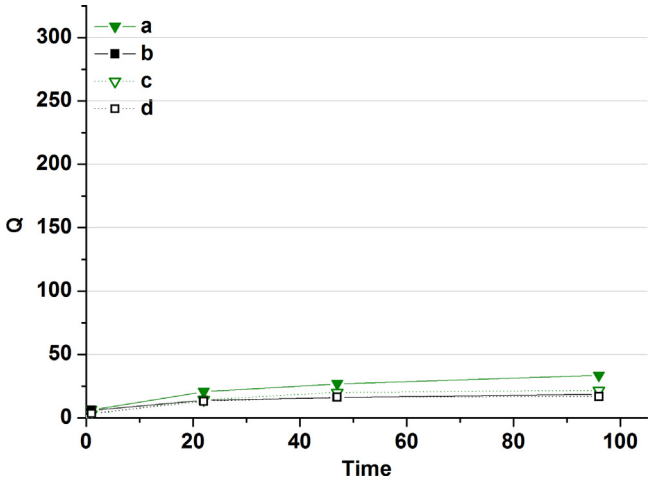

Fig. 9. Swelling curves of SWH2-based hydrogels in deionized water comprised of (a) SWH2-al$_{29}$/1b, (b) SWH2-al$_{29}$/3b, (c) SWH2-al$_{27}$/1b, (d) SWH2-al$_{27}$/3b.

was extended to 14, 20 and 40 h. The degree of substitution and the nomenclature of the samples are presented in Table 4.

Considering the reaction times, and by comparing the calculated degrees of substitution for SWH2 to the obtained degrees of substitution for SWH1, it is noticeable that SWH2 has lower reactivity. This lower reactivity is a result of the higher lignin content and the lower content of mono-sugars such as mannose and glucose in SWH2, leading to a maximum degree of substitution approximately 0.28.

The modified SWH2 species were used as substrates for hydrogel preparation using initiator *b*, and formulated as stated in Table 1. The attained hydrogels were cylindrical and dark brown, due to the lignin present in the original SWH2. Fig. 9 shows the swelling curves of the two hydrogel compositions produced from SWH2-al$_{29}$ and SWH2-al$_{27\text{-}1}$. All SWH2 hydrogel formulations displayed considerably lower equilibrium swelling values in comparison with SWH1 hydrogels of analogous formulations. This is due to the larger amount of lignin accompanying the hydrophilic hemicellulose chains relative to SWH1, which can give rise to the existence of hydrophobic domains within the gel structure and thus reduce hydrophilicity.

4. Conclusions

A pathway for the conversion of non-purified, lignin-containing and hemicellulose-rich wood hydrolysate into highly swelling hydrogels was developed and demonstrated. Allyl-modification of SWH1, a side stream of pre-hydrolysis kraft cooking for dissolving pulp, efficiently introduced a sufficient number of allyl-sites onto the backbone of SWH acetyl galactoglucomannan and was tunable by varying the reaction time. Two different redox initiator systems comprised of either KPS (*a*) or APS (*b*) were evaluated for hydrogel synthesis. Modified SWH1s were successfully converted to highly swellable hydrogels with equilibrium swelling values ranging from Q_{eq} = 50 to 270. The storage moduli of all hydrogels were remarkably larger than their loss moduli, indicating a dominant elastic response of the hydrogels. DMTA investigations were also used to elaborate the effect of the initiator system on the cross-link density of the hydrogels. In accordance with the swelling and DMTA assessments, hydrogels of varying properties can be achieved from less substituted SWH1 and using initiator *a*, which is more economically feasible for industrial applications. The developed hydrogel production pathway was also applicable to other wood hydrolysates, as demonstrated by using the non-purified press water from fiberboard production to produce hydrogels. The high degree of swelling of the SWH1 hydrogels is an appreciable property for applications such as absorbing materials, drying agents, or water retaining agents with agricultural end use.

Acknowledgements

We thank FORMAS (project number 2011-1542) for financial support. Therese Tyson (Redin) is acknowledged for her contribution in the synthesis of SWH2-based hydrogels.

Appendix A. Supplementary data

Supplementary data associated with this article can be found, in the online version, at http://dx.doi.org/10.1016/j.carbpol.2014.02.060.

References

Albertsson, A.-C., Voepel, J., Edlund, U., Dahlman, O., & Söderqvist-Lindblad, M. (2010). Design of renewable hydrogel release systems from fiberboard mill wastewater. *Biomacromolecules*, *11*(5), 1406–1411.
Anseth, K. S., Bowman, C. N., & Brannon-Peppas, L. (1996). Mechanical properties of hydrogels and their experimental determination. *Biomaterials*, *17*(17), 1647–1657.
Dahlman, O., Söderqvist Lindblad, M., Parkås, J., Albertsson, A.-C., & Edlund, U. (2009). *Utilization of a wood hydrolysate*.
EDANA, G. o. (2012). *Standard test: WSP 241.2.R3 gravetimetric determination of fluid retention capacity in saline solution after centrifugation*.
Edlund, U., & Albertsson, A.-C. (2008). A microspheric system: hemicellulose-based hydrogels. *Journal of Bioactive and Compatible Polymers*, *23*(2), 171–186.
Edlund, U., Ryberg, Y. Z., & Albertsson, A.-C. (2010). Barrier films from renewable forestry waste. *Biomacromolecules*, *11*(9), 2532–2538.
Edlund, U., Svensson, M., & Albertsson, A.-C. (2012). Microsphere valorization of forestry derived hydrolysates. *European Polymer Journal*, *48*(2), 372–383.
Hartman, J., Albertsson, A.-C., Lindblad, M. S., & Sjöberg, J. (2006). Oxygen barrier materials from renewable sources: Material properties of softwood hemicellulose-based films. *Journal of Applied Polymer Science*, *100*(4), 2985–2991.
Hossein, O., & Kinam, P. (2010). Introduction to hydrogels. In O. M. Raphael, P. Kinam, & O. Teruo (Eds.), *Biomedical applications of hydrogels handbook*. New York: Springer.
Ibn Yaich, A., Edlund, U., & Albertsson, A.-C. (2011). Wood hydrolysate barriers: performance controlled via selective recovery. *Biomacromolecules*, *13*(2), 466–473.
Kuzmenko, V., Hägg, D., Toriz, G., & Gatenholm, P. (2013). In situ forming spruce xylan-based hydrogel for cell immobilization. *Carbohydrate Polymers*, *102*, 862–868.
Mittal, K. L., & Anderson, H. R. (2000). *Acid–base interactions: relevance to adhesion science and technology*. Utrecht: VSP.
Mun, G., Suleimenov, I., Park, K., & Omidian, H. (2010). Superabsorbent hydrogels. In R. M. Ottenbrite, K. Park, & T. Okano (Eds.), *Biomedical applications of hydrogels handbook* (pp. 375–391). New York: Springer.
Pahimanolis, N., Sorvari, A., Luong, N. D., & Seppälä, J. (2013). Thermoresponsive xylan hydrogels via copper-catalyzed azide-alkyne cycloaddition. *Carbohydrate Polymers*, *102*, 637–644.
Persson, T., Matusiak, M., Zacchi, G., & Jönsson, A.-S. (2006). Extraction of hemicelluloses from process water from the production of masonite. *Desalination*, *199*(1–3), 411–412.
Ragauskas, A. J., Williams, C. K., Davison, B. H., Britovsek, G., Cairney, J., Eckert, C. A., et al. (2006). The path forward for biofuels and biomaterials. *Science*, *311*(5760), 484–489.
Saadatmand, S., Edlund, U., Albertsson, A.-C., Danielsson, S., & Dahlman, O. (2012). Prehydrolysis in softwood pulping produces a valuable biorefinery fraction for material utilization. *Environmental Science & Technology*, *46*(15), 8389–8396.
Saadatmand, S., Edlund, U., Albertsson, A.-C., Danielsson, S., Dahlman, O., & Karlström, K. (2013). Turning hardwood dissolving pulp polysaccharide residual material into barrier packaging. *Biomacromolecules*, *14*(8), 2929–2936.
Sixta, H. (2006). *Chemical pulping. Handbook of pulp*. Weinheim: WILEY-VCH.

Socrates, G. (2001). *Infrared and Raman characteristic group frequencies: tables and charts*. Wiley.

Sun, X.-F., Wang, H.-H., Jing, Z.-X., & Mohanathas, R. (2013). Hemicellulose-based pH-sensitive and biodegradable hydrogel for controlled drug delivery. *Carbohydrate Polymers*, *92*(2), 1357–1366.

Söderqvist Lindblad, M., Albertsson, A.-C., Ranucci, E., Laus, M., & Giani, E. (2005). Biodegradable polymers from renewable sources: Rheological characterization of hemicellulose-based hydrogels. *Biomacromolecules*, *6*(2), 684–690.

Söderqvist Lindblad, M., Ranucci, E., & Albertsson, A.-C. (2001). Biodegradable polymers from renewable sources. New hemicellulose-based hydrogels. *Macromolecular Rapid Communications*, *22*(12), 962–967.

TAPPI. (2009). *Carbohydrate composition of extractive-free wood and wood pulp by gas–liquid chromatography, Test Method T 249 cm-09*. Atlanta: TAPPI Press.

TAPPI. (2011). *Acid-insoluble lignin in wood and pulp. Test Method T 222 om-11*. Atlanta: TAPPI Press.

Voepel, J., Edlund, U., & Albertsson, A.-C. (2009). Alkenyl-functionalized precursors for renewable hydrogels design. *Journal of Polymer Science Part A: Polymer Chemistry*, *47*(14), 3595–3606.

Yaich, A. I., Edlund, U., & Albertsson, A.-C. (2014). Adapting wood hydrolysate barriers to high humidity conditions. *Carbohydrate Polymers*, *100*(0), 135–142.

Zhu Ryberg, Y. Z., Edlund, U., & Albertsson, A. C. (2011). Conceptual approach to renewable barrier film design based on wood hydrolysate. *Biomacromolecules*, *12*(4), 1355–1362.